Modeling of Revitalization of Atmospheric Water

Robert Coker[*1] and Jim Knox[1]
[1]Marshall Space Flight Center, NASA
*Corresponding author: ES22, MSFC, Huntsville, AL 35812, robert.f.coker@nasa.gov

Abstract: The Atmosphere Revitalization Recovery and Environmental Monitoring (ARREM) project was initiated in September of 2011 as part of the Advanced Exploration Systems (AES) program. Under the ARREM project, testing of sub-scale and full-scale systems has been combined with multiphysics computer simulations for evaluation and optimization of subsystem approaches. In particular, this paper describes the testing and modeling of the water desiccant subsystem of the carbon dioxide removal assembly (CDRA). The goal is a full system predictive model of CDRA to guide system optimization and development.

Keywords: adsorption, flow, thermal transport, validation.

1. Introduction

Predictive simulation tools are being developed to reduce the hardware testing requirements of the ARREM project as part of NASA's AES program[1,2]. Although sub-scale testing is required to establish the predictive capability of the simulations, the much greater cost of extensive full-scale testing can be limited to that required for the confirmation of analytical design optimization studies. Once predicative capability is established, geometric reconfiguration of a model is usually straightforward. A predictive simulation capability provides improved understanding of complex processes since process conditions (temperature, pressure, concentrations, etc.) may be examined anywhere in the sorption column. Weaknesses in a prototype design can be readily identified and improvements tested via simulation. Finally, the predictive simulation provides a powerful tool for virtual troubleshooting of deployed flight hardware.

Here, we discuss using the COMSOL Multiphysics code[3] to model in detail – and predictively – experiments that are similar to the desiccant subcomponent of a full CDRA system.

Adsorption in packed fixed beds of pelletized sorbents is presently the primary means of gas separation for atmosphere revitalization systems. However, structured sorbents are emerging as a new approach to sorbent systems. Structured sorbents are produced as monoliths, with an open structure for airflow, or by fixing sorbents on an inert substrate such as paper-like honeycomb structures or expanded metal sheets. An accurate assessment of structured sorbents and comparison with packed bed designs is desirable; experimental results so far show unanticipated variation in packed bed breakthrough for identical beds held under the same conditions. It is suspected that small packing irregularities can propagate downstream in large beds and impact process efficiency. This indicates a margin of error inherent in packed bed fabrication and thus a likely superiority of structured sorbents for

Figure 1. CBT test stand.

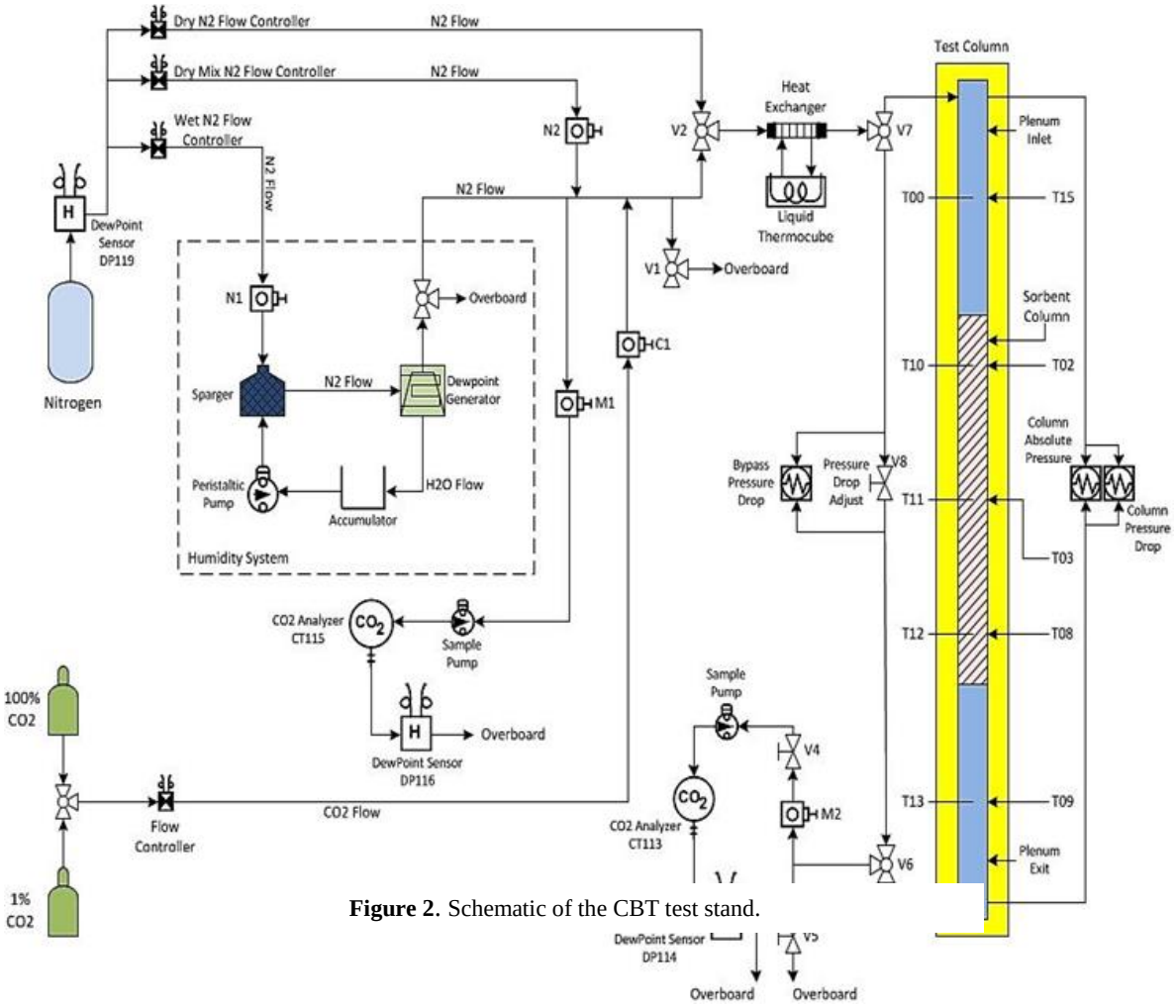

Figure 2. Schematic of the CBT test stand.

process efficiency and control. This paper discusses fully predictive modeling results using COMSOL's Multiphysics code for a geometrically simple fixed bed design. Insights learned from this work will be used in future modeling of the entire CDRA system.

For the bulk separation of CO_2 and H_2O, temperature changes due to the heat of adsorption are significant, requiring the simulation of the heat balance equations through the beds and the housing, as well as the equations for sorption processes and fluid flow. For columns with small tube diameter to pellet diameter ratios, as encountered in internally heated columns, flow channeling along the column wall can have a strong influence on overall performance. Here, with over a dozen pellets per cylinder diameter, 1-D models should prove accurate enough for predictively driven system design.

2. Cylindrical Breakthrough Test

2.1 Description

The CDRA requires a water-saving bulk drying stage prior to downstream CO_2 removal. The primary goal is to continuously remove at least 80% and up to 100% of water vapor from a process air stream. The Cylindrical Breakthrough Test (CBT) was constructed to compare sorption kinetics for various sorbent and sorbate pairs. The tests consist of flowing a constant amount of sorbate and carrier gas through a fixed bed containing a regenerated (or dried out) sorbent. After some period of time (the 'breakthrough time'), the sorbate is detected at the bed exit. A plot of the sorbate concentration or partial pressure versus time is the breakthrough curve. Axially routed thermocouples are used to acquire temperature curves inside and outside of the bed as well as

before and after the packed bed. The three thermocouples inside the bed are on axis and are located 1 inch inside the inlet and exit and in the axial middle of the sorbent-filled bed. Absolute and differential pressure is measured at the column inlet and across the column, respectively.

The test apparatus, shown in Fig. 1, was designed to have relatively low mass (to reduce regeneration time) and good axial symmetry (to reduce system complexity). The test bed, packed with regenerated sorbent pellets, is insulated to minimize system heat loss. Mass flow controllers are used to blend N_2, the carrier gas, with the desired partial pressure of CO_2 or H_2O. For CO_2 tests, Sable Systems CO_2 analyzers provide inlet and outlet CO_2 partial pressure readings, while for H_2O tests, a Sable Systems Dew Point Generator provides humidity control and Edgetech Dewmaster dew point analyzers provide inlet and outlet dew point measurements. A schematic of the entire test setup is shown in Fig. 2. The cylindrical column of sorbent has a bed length, *B*, of 16.51 cm and a radius, R_B, of 1.74 cm. The mass of regenerated sorbent in the test bed is measured so as to determine the mean porosity of the bed. The Al 6061 housing is *d*=0.065 inches thick and extends for 6 inches upstream and downstream of the sorbent. The sorbent is held in place inside the housing using spring-loaded plates and fine mesh screens. Here, we focus on the CBT adsorption tests, where the sorbent starts fully regenerated. Experimental data from the CBT will be used to validate the simulation process so that simulation-driven optimization may be used alongside conventional design methods to perfect CDRA sub-component design and testing.

2.2 Models

1-D models of the CBT were constructed using the COMSOL Multiphysics code using Domain ODEs and DAEs. Only the sorbent-containing part of the bed is modeled. A constant porosity, ϵ, was used, such that, together with the known constant density of the dry sorbent pellets, ρ_s, the proper measured total sorbent mass is recovered. Using the measured mean particle diameter of the sorbent pellets, D, the local permeability within each cell is then found[4]:

$$\kappa = \frac{\epsilon^{5.5}\kappa_f D^2}{5.6} \quad (1).$$

However, the correct diameter to use in Eq.(1) is a volume-weighted averaged such as the Sauter mean, but this is not as well-known as D for all sorbents, but it is generally larger than D. The factor, κ_f, is adjusted to reproduce the measured pressure drop through the test bed for a given test (so it is not a free parameter). Eq.(1) was developed for typical sandstone packing, while some sorbents are very spherical and smooth. Further, in 1-D the use of a constant porosity in Eq. (1) will over-estimate the center-line permeability, so values of κ_f less than unity are typical.

A 1-D PDE for the interstitial fluid flow velocity, *u*, is derived based on a simplification of the Navier-Stokes and Brinkman equations while assuming compressible flow; this is combined with PDEs for the loading, *q*, based on the Toth equations, the sorbate concentration, *c*, and the temperature of the gas mixture (T_g), sorbent pellets (T_s), and housing walls (T_c). Note that COMSOL flow modules (not used here) all solve for the *superficial* velocity (=ϵu). The interstitial velocity is found via Eq (2), where *P* is the total gas pressure of the carrier gas and sorbate mixture, ρ_g is the density of the gas mixture, *A* is the ratio of sorbent area to volume (see below), μ_g is the mixture gas viscosity, and M_a is the mean molecular mass of the sorbate. Eq.(2) is essentially a 2nd order Ergun[5] equation that reduces to Darcy's Law in steady state and in the limit of a zero velocity gradient and no sorption. The 2nd order Ergun term, proportional to the square of the fluid velocity, is somewhat akin to a Forchheimer drag term. The $\frac{\partial q}{\partial t}$ term

$$\rho_g \frac{\partial u}{\partial t} - \frac{\partial}{\partial x}\left(\frac{\mu_g}{\epsilon}\frac{\partial(\epsilon u)}{\partial x}\right) = -\left(\frac{\partial P}{\partial x} + u\left(\frac{\epsilon\mu_g}{\kappa} + \epsilon^2|u|\rho_g A + \frac{\partial q}{\partial t}\frac{(1-\epsilon)}{\epsilon}M_a + \rho_g\frac{\partial u}{\partial x}\right)\right) \quad (2),$$

compensates for the transfer of momentum from the overall flow to the stationary sorbent. In COMSOL, the entirety of the RHS of Eq.(2) is written as a source term in the General Form PDE; the pressure gradient cannot be written as a flux term or the combined boundary conditions become over-constrained. Thus, the boundary conditions applied to Eq. (2) are simply $\left.\frac{\partial u}{\partial x}\right|_{x=0} = \left.\frac{\partial u}{\partial x}\right|_{x=B} = 0$. Eq.(2) assumes the ideal

gas law for the density of the gas mixture, so that:

$$\rho_g = \frac{P}{R_s T_g} \quad (3),$$

where the mixture's specific gas constant is given by $R_s = R_g/M_{mix}$. The mean molecular mass of the gas mixture is $M_{mix} = M_N + R_g T_g c(M_a - M_N)/P$, where M_N is the molecular mass of the pure carrier gas, generally N_2.

The second PDE solves for the total gas pressure, P, using the continuity equation and Eq.(3):

$$\frac{\epsilon}{R_s T_g}\frac{\partial P}{\partial t} + \frac{\partial}{\partial x}\left(\frac{\epsilon u P}{R_s T_g}\right) + P\frac{\partial\left(\frac{\epsilon}{R_s T_g}\right)}{\partial t} = -\frac{\partial q}{\partial t}(1-\epsilon)M_a \quad (4).$$

In COMSOL, in the Coefficient Form PDE, the 1st term of Eq.(4) is a Damping term, the 2nd is a Conservative Flux term, and the 3rd is an Absorption term, while the RHS is a source term accounting for the change in total pressure as sorption proceeds. The outlet pressure boundary condition is of the Dirichlet type, using the measured outlet pressure from a given test, $P_{out} = P_{in} - \Delta P$. The inlet uses a mass flux boundary condition based on the measured constant standard flow rate, F, for a given test:

$$\rho_g \epsilon u|_{x=0} = f_M = \frac{P_0}{R_s T_0}\frac{F}{A_f} \quad (5),$$

where $A_f = \pi R_B^2$ is the inlet free flow area and P_0 and T_0 are the reference pressure and temperature, respectively, at which the flowrate is defined. Thus, the 1st term of the RHS in Eq.(5) is a reference density. Here, P_0=1 atm and T_0=0°C. Since this is a 1-D 'plug flow' model, there is no gradient of pressure, velocity, concentration, temperature, or porosity in the radial direction, although out-of-plane thermal effects are taken into account (see below).

The third and fourth PDEs are coupled and solve for sorb

ate concentration, c, and pellet loading, q, respectively. The latter applies the Linear Driving Force model[6]. Together these two PDEs are referred to as the 'Mass Balance' equations. The General Form PDEs are:

$$0 = \epsilon\frac{\partial c}{\partial t} + (1-\epsilon)\frac{\partial q}{\partial t} + \frac{\partial}{\partial x}\left(u\epsilon c - D_x\frac{\partial c}{\partial x} - D_x\frac{c}{M_{mix}}\frac{\partial M_{mix}}{\partial x} + D_x\frac{c}{\rho_g}\frac{\partial \rho_g}{\partial x}\right) \quad (6)$$

$$\frac{\partial q}{\partial t} = k_m(q_* - q) \quad (7),$$

where D_x is the local time-dependent axial mass dispersion coefficient, q_* is the equilibrium loading from the Toth isotherms, and k_m is the constant mass transfer coefficient (see below). For the concentration, a zero gradient mass concentration Constraint:

$$\left.\frac{\partial c}{\partial x}\right|_{x=B} - \left.\frac{c}{\rho_g}\frac{\partial \rho_g}{\partial x}\right|_{x=B} = 0 \quad (8),$$

is used at the exit, while a molar volume flux boundary condition is used at the inlet:

$$D_x\left(\left.\frac{\partial c}{\partial x}\right|_{x=0} - \left.\frac{c}{\rho_g}\frac{\partial \rho_g}{\partial x}\right|_{x=0} - \left.\frac{c}{M_{mix}}\frac{\partial M_{mix}}{\partial x}\right|_{x=0}\right) = \epsilon u_{in} c_{in} \quad (9),$$

where $u_{in} = f_M R_s T_{gin}(t)/P_{vapin}(t)$, is the inlet interstitial velocity and $c_{in} = P_{vapin}(t)/R_g/T_{gin}(t)$, is the sorbate concentration at the upstream inlet to the bed. $P_{vapin}(t)$ and $T_{gin}(t)$ are the measured time-dependent sorbate partial pressure and gas temperature, respectively, for each experiment. Since $T_{gin}(t)$ is measured far upstream of the start of the sorbent in the bed, the COMSOL inlet value is the measured value minus an offset due to losses or gains along the uninsulated piping. That is, this ensures that $T_{gin}(t=0)$ actually equals the $T_g(t=0,x=0)$ inside the bed for any given experiment. There are no explicit spatial boundary conditions required for Eq.(7) since there is no loading outside of the sorbent bed. In COMSOL, it is necessary to make all of the gradient terms of Eq.(6) a flux term, in order to apply the inlet flux boundary condition of Eq. (9) properly. The above transport PDE, Eq.(6), represents Fickian diffusion[6] in conservative form and assumes that all mechanical dispersion effects are lumped together with molecular diffusion in the axial dispersion term. Note that together Eqs. (2), (4), and (6) model the transport of a concentrated species. That is, M_{mix} is not assumed to be constant and the density gradient of the carrier gas can have an effect on the sorbate concentration.

$$(1-\epsilon)\rho_s c_{ps}\frac{\partial T_s}{\partial t}+\frac{\partial}{\partial x}\left(-k_s(1-\epsilon)\frac{\partial T_s}{\partial x}\right)=\mathrm{A}h_{sg}\left(T_g-T_s\right)-\partial\mathrm{H}(1-\epsilon)\frac{\partial q}{\partial t} \quad (10)$$

$$\epsilon\rho_g c_{pg}\frac{\partial T_g}{\partial t}+\frac{\partial}{\partial x}\left(-k_{gx}\epsilon\frac{\partial T_g}{\partial x}\right)=\mathrm{A}h_{sg}\left(T_s-T_g\right)-\epsilon\rho_g c_{pg}u\frac{\partial T_g}{\partial x}+\frac{P_I h_{gc}\left(T_c-T_g\right)}{A_f} \quad (11)$$

$$\rho_c c_{pc}\frac{\partial T_c}{\partial t}+\frac{\partial}{\partial x}\left(-k_c\frac{\partial T_c}{\partial x}\right)=\frac{P_I h_{gc}\left(T_g-T_c\right)}{A_c}+\frac{P_O h_{Ac}\left(T_A-T_c\right)}{A_c} \quad (12).$$

The fifth, sixth, and seventh PDEs are coupled and solve for the sorbent temperature, the gas temperature, and the wall housing temperature, respectively. Together these are referred to as the 'Thermal Balance' equations. Since the sorbent pellets and sorbate plus carrier gas are not in thermal equilibrium, the COMSOL Heat Transfer module is insufficient and explicit PDEs are needed. The General Form PDEs are given in Eqtns (10-12).

All of the terms on the RHS of Eqs.(10-12) are source terms in COMSOL, with the perimeter terms corresponding to out-of-plane convective flux terms. Since u_s and u_w are identically zero everywhere (thus, $u \equiv u_g$), zero flux boundary conditions are used for Eqs.(10 and 12):

$$\left.\frac{\partial T_c}{\partial x}\right|_{x=0}=\left.\frac{\partial T_c}{\partial x}\right|_{x=B}=\left.\frac{\partial T_s}{\partial x}\right|_{x=0}=\left.\frac{\partial T_s}{\partial x}\right|_{x=B}=0.$$

In Eqs.(10-12), subscripts *s*, *g*, *A*, and *c* refer to properties of the sorbent, gas mixture, ambient environment, and can housing, respectively. $P_I = 2\pi R_B$, $P_O = 2\pi(R_B+d)$, and $A_c = \pi((R_B+d)^2 - R_B^2)$ are the can inner perimeter, outer perimeter, and cross sectional area, respectively. Heat capacity, thermal conductivity, and thermal transfer coefficients are given by c_p, k, and h, respectively. The heat of adsorption for a given sorbate/sorbent pair is given by $\partial\mathrm{H}$ and is a (poorly known) function of q and T_s (see Table 1 below). The ratio of sorbent area to volume assumes spherical pellets and is given by $\mathrm{A} = (1-\epsilon)6A_f/D$. The outlet boundary condition for Eq.(11) is given by a zero gradient Constraint:

$$\left.\frac{\partial T_g}{\partial x}\right|_{x=B}=0 \quad (13),$$

while the inlet is given by a flux boundary condition:

$$\epsilon k_{gx}\left.\frac{\partial T_g}{\partial x}\right|_{x=0}=\rho_g c_{pg}\epsilon u\left(\mathrm{T}_{gin}(t)-T_g\right) \quad (14).$$

The void fraction is left explicitly in Eq. (14) to illustrate that in COMSOL, one must be careful to define boundary conditions that are consistent with any Conservative Flux terms. In the limit of $T_s = T_g$, Eqs. (10-14) are the same equations as given in a combined Heat Transfer in Solids and Porous Media COMSOL module that is set up with heat sources and out-of-plane convective heat flux nodes.

The initial conditions for the *c* and *q* PDEs correspond to equilibrium loading for a small initial sorbate partial pressure, typically 1-5 Pa. The initial velocity is u_{in} everywhere, while the initial pressure is set to $P_{in}-\Delta P^* x/B$. All temperatures are initially linear so as to start with the measured (but offset) $\mathrm{T}_{gin}(t=0)$ at x=0 and $\mathrm{T}_{gout}(t=0)$ at $x=B$.

The boundary conditions described above for *P*, *T*, and *c* are all the measured values from a given test, with *T* and *c* being time-dependent. This is necessary since, as will be seen below, the variation from test to test (or even within a single test), even using the same packed bed and nominal test conditions for flow rate and inlet sorbate partial pressure, is often larger than the uncertainty in the model.

2.2.1 *Dimensionless Numbers*

Many of the physical parameters used in Eqs.(10-12) are determined from correlations based on dimensionless quantities. The empirical relationships used here are appropriate for 1-D models in the regime of the CBT. The Schmidt number, *Sc*, pellet Reynolds number, *Re*, Peclet number[7], *Pe*, Prandtl number, *Pr*, gas to sorbent Nusselt number, Nu_{GS}[8], and gas to can Nusselt number, Nu_{GC}[9], are given by:

$$Sc=\frac{\mu_g}{\rho_g D_{AB}} \quad (15)$$

$$Re=\frac{u\rho_g D}{\mu_g} \quad (16)$$

$$\frac{1}{Pe_{(x,r)}} = \frac{0.73\epsilon}{ReSc} + \frac{1}{f_{(x,r)}\left(1 + \frac{13 * 0.73\epsilon}{ReSc}\right)} \quad (17)$$

$$Pr = \frac{\mu_g c_{pg}}{k_g} \quad (18)$$

$$Nu_{GS} = 2 + 1.1\ Pr^{1/3} Re^{0.6} \quad (19)$$

$$Nu_{GC} = 2.63\ Re^{0.8} e^{-3D/R_B} \quad (20).$$

In Eq.(17), $f_{(x,r)}$ is 2 for axial (Pe_x) and 10 for radial (Pe_r) parameters. In Eq.(15), D_{AB} is the binary mass diffusion coefficient[10] for either water vapor or carbon dioxide in N_2 or air (the carrier gas) as a function of P and T_g

2.2.2 *Toth Isotherms*

The loading equation uses the Toth isotherm relationships:

$$q_* = \frac{\rho_s a P_{vap}}{\left(1 + \left(b P_{vap}\right)^{t_T}\right)^{1/t_T}} \quad (21)$$

$$b = b_0 e^{E/T_g} \quad (22)$$

$$a = a_0 e^{E/T_g} \quad (23)$$

$$t_T = t_0 + \frac{c_0}{T_g} \quad (24),$$

where $P_{vap} = c\ R_g\ T_g$ is the sorbate partial pressure and a_0, b_0, t_0, c_0, and E are Toth coefficients for a given sorbent/sorbate pair. The coefficients used[12] are listed in Table 1, together with the heat of adsorption[12,13] for each pair. It is known that ∂H depends on loading, decreasing significantly in magnitude as equilibrium loading is approached as well as when the sorbent is colder; the quantitative dependence, however, is not well known for many sorbents. A crude 2nd order in loading and 1st order in temperature fit to data for most sorbent/sorbate pairs was done at MSFC; only CO_2 on SG is missing. The other ∂H values listed in Table 1 are for a sorbent temperature of 12.5ºC and a specific loading of 1 mol/kg. For the silica gel sorbents, Grace Grade 40 and Sylobead B125, the same Toth parameters are used, even though they are experimentally derived from the former. The same is true for the 5A zeolite sorbents, Grace Grade 522 and RK-38. There are no CBT experiments as yet with H_2O/5A or CO_2/SG systems.

2.2.3 *Material Properties*

Some material properties are from COMSOL's material libraries and some use the correlations in the previous section. Temperatures in the following expressions are in Kelvin and the derived values are in MKS units.

The axial mass dispersion coefficient used in Eq.(6) for the transport of the sorbate through the bed is given by:

$$D_x = \frac{uD}{Pe_x} (25).$$

while for the carrier gas, COMSOL expressions for N_2 are used. For the can properties, COMSOL functions for Al 6061 are used. Also from the COMSOL material library, the heat capacity, viscosity, and thermal conductivity of water vapor or carbon dioxide, as appropriate, were used for the sorbate.

$$k_{gx} = c_{pg} \rho_g D_x \quad (26)$$

The effective axial gas thermal conductivity, k_{gx}, comes from a similarity assumption[6], which may not be valid in all regimes. The resulting values are typically as much as 50% larger than when using other, more complicated expressions[14]; the impact of different k_{gx} expressions on the breakthrough curves discussed here is minor. Note that k_{gx} depends on the gas mixture heat capacity (see below).

For the sorbent properties, since they are not well known, constant values are used[12,15,16].

Table 1. Adsorption Parameters for Sorbent/Sorbate Pairs

Sorbate/Sorbent System	a_0 mol kg^{-1} kPa^{-1}	b_0 kPa^{-1}	E K	t_0	c_0 K	∂H kJ mol^{-1}
CO_2/5A	9.875x10^{-7}	6.761x10^{-8}	5.625x10^{3}	2.700x10^{-1}	-2.002x10^{1}	-39.9
H_2O/5A	1.106x10^{-8}	4.714x10^{-10}	9.955x10^{3}	3.548x10^{-1}	-5.114x10^{1}	-60.5
CO_2/13X	6.509x10^{-3}	4.884x10^{-4}	2.991x10^{3}	7.487x10^{-2}	3.805x10^{1}	-36.8
H_2O/13X	3.634x10^{-6}	2.408x10^{-7}	6.852x10^{3}	3.974x10^{-1}	-4.199	-56.7
CO_2/SG	7.678x10^{-6}	5.164x10^{-7}	2.330x10^{3}	-3.053x10^{-1}	2.386x10^{2}	-40.0
H_2O/SG	1.767x10^{2}	2.787x10^{-5}	1.093x10^{3}	-1.190x10^{-3}	2.213x10^{1}	-36.8

They are listed for the sor[illegible] an is less coupled to the flow.

Table 2. Properties of Sorbents as Packed in the CB

Sorbent	ρ_s kg m^{-3}	c_{ps0} (@26°C) J kg^{-1} K^{-1}	k_s W m^{-1} K^{-1}	$D_{pellets}$ mm	mass g	ϵ
5A (Grace Grade 522)	1190	750	0.152	2.22	125.0	0.331
5A (RK38)	1370	650	0.144	2.10	119.3	0.445
13X (Grace Grade 544)	1260	800	0.147	2.19	107.4	0.457
SG (Grace Grade 40)	1240	870	0.165	2.90	111.7	0.415
SG (Sylobead B125)	1240	870	0.151	2.25	127.0	0.348

in Table 2. For Sylobead B152, the sorbent density and heat capacity are assumed to be the same as for Grace Grade 40. Also listed in Table 2 are the mean pellet diameter, total dry sorbent mass, and resulting mean porosity for the sorbent packings used in the CBT experiments.

The gas mixture quantities are calculated using a mass-fraction weighting between the carrier gas and the sorbate gas. The sorbate mass fraction, f_a is given by $c\, M_a / \rho_g$ while the carrier mass fraction, f_N, is 1- f_a.

The heat capacity of the pellets can change significantly as they get loaded. Thus, a mass-weighted loading-dependent effective heat capacity is used for c_{ps}:

$$c_{ps} = \frac{\left(c_{p(H2O,CO2)}\, qM_{(H2O,CO2)} + c_{ps0}\rho_s\right)}{\left(qM_{(H2O,CO2)} + \rho_s\right)} \quad (27).$$

Eq.(39) typically reduces the pellet heat capacity by ~10% when the sorbate is H_2O, but is insignificant for CO_2.

The thermal transfer coefficients for the gas are determined from *Nu*:

$$h_{sg} = Nu_{GS} k_g / D \quad (28)$$

$$h_{gc} = \frac{Nu_{GC} k_g}{(2R_B)} \quad (29),$$

while for the ambient-to-can heat transfer, a nominal constant small value of h_{Ac}=0.1 W/m^2/K was used, since the insulation was not firmly bonded with the cylinder. As a result, the value used for T_A, the ambient temperature, is not very critical, so a constant 19°C value, representative of the CBT laboratory, was used in this work. However, when available T_A was set to the measured value for each test, resulting in slightly improved late time temperature profiles (see below). Also, h_{sg} is typically ~150 W/m^2/K, so the gas and sorbent are moderately well thermally coupled, while h_{gc} is typically ~50 As a result, in the results discussed below, typically,$|T_g$-$T_s|$ <<1°C and $|T_g$-$T_c|$ >>1°C

3. COMSOL Results

The only free parameter required to fit the CBT data is k_m, the mass transfer coefficient used in the LDF model (see Eq.(7)). It is not expected to be sensitive to different test conditions, such as flow rates, vapor pressure, or temperatures. Ideally, it is only a function of the sorbent/sorbate pairing, but in practice it can vary due to, for example, geometry differences when R_B is only a few times D, making arbitrary predictive applications with the LDF model problematic. Here, the same value of k_m is used for all CBT experiments of a given sorbent/sorbate pairing. Note that k_m drives the slope of the vapor pressure rise curve, so for the model to be self-consistent, it should reproduce that slope; that is, even k_m is not a true free parameter even for a single test of a given sorbent/sorbate pairing. The intent is to derive k_m for a given sorbent/sorbate pair and use it in future predictive modeling of CDRA-related systems. It is to be emphasized that once k_m is determined for a given test of a sorbate/sorbent system, the other tests of that sytem (at different flow rates and partial pressures) are predictively modeled.

The COMSOL results for the predicted and experimentally measured exit temperatures and vapor pressures for some illustrative sorbent/sorbate pairs are shown in figures 3-6. The derived values of k_m used for the various sorbent/sorbate systems are listed in Table 3. It can be seen that k_m varies by a factor of 5, with 0.002 s^{-1} being a typical value.

Table 3. COMSOL Mass Transfer Coefficients

Sorbent/Sorbate System	k_m (s^{-1})
Sylobead/H_2O	0.002
Grade 40/H_2O	0.00125
Grade 544/H_2O	0.0007
RK38/CO_2	0.003
Grade 522/CO_2	0.0035

3.1. H_2O on Silica Gel Grade 40

Two flow rates, 16 SLPM and 8 SLPM, and two inlet partial pressures, corresponding to dew points of 0.5°C and 10°C, were run with silica gel Grace Grade 40 sorbent. The two flow rates correspond to Reynolds numbers of ~150 and ~70, respectively. Figs. 3 and 4 show the temperatures and vapor pressures for the 16 SLPM and 0.5°C dew point case. The COMSOL peaks are too low and they fall off too slowly, particularly close to the inlet. Also, the late time temperatures do not separate as they do in the data. The COMSOL vapor pressure rise matches the data well, only missing some of the complexity of the curve shape. This is likely due to a combination of the simplicity of the LDF model and inaccuracies in the dew point data. The partial pressure results show that the data at late times do not approach the inlet values; the reason for this consistent deficiency is unknown but may be related to calibration issues with the dew point sensors, since it does not occur in the CO_2 tests (see below).

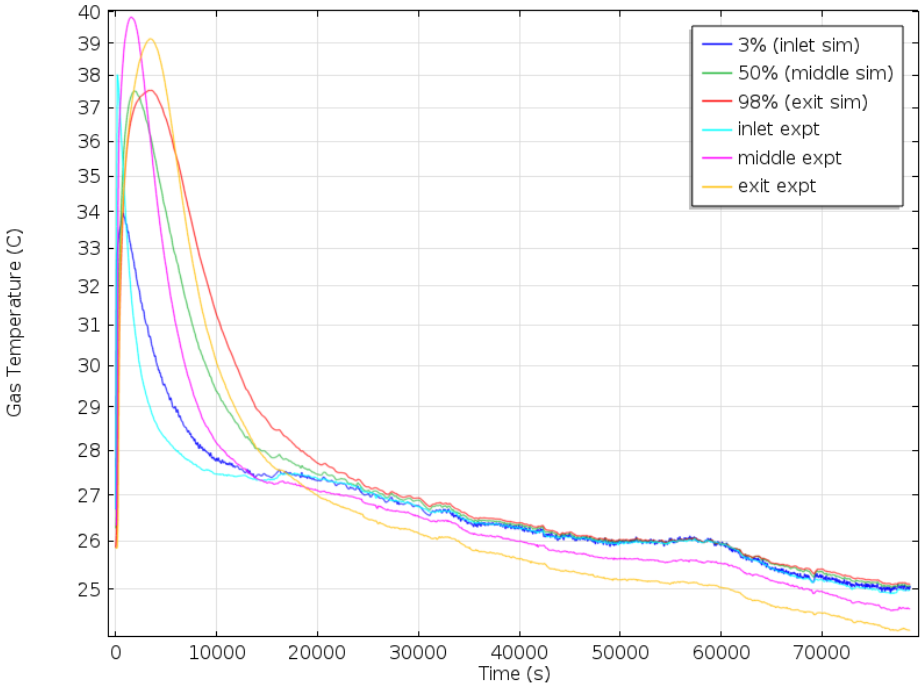

Figure 3. Temperatures for SG Grade 40 with 16 SLPM and 0.5°C dew point.

3.5 CO_2 on 5A Zeolite RK38

Two flow rates, 16 and 8 SLPM, and two inlet partial pressures, 2.5 and 5.0 Torr, were run for CO_2 on RK38. Temperature and partial pressure comparisons between the experiments and the COMSOL models for the 16 SLPM 5 Torr case are shown in Figs. 5 and 6, respectively. As for the SG results, the model peak temperatures are too low and fall off too slowly. This suggests that issues with the thermal transport in general (such as the correlation-derived thermal transfer coefficients given above) are more likely the problem than sorbent-specific properties such as the heat of adsorption. Fig. 6 shows that the COMSOL model matches the breakthrough curve quite well.

The adsorption capacity, the moles of sorbate per unit mass of sorbent that the system can adsorb, was measured to be 1.18±0.05 mol/kg. In the models, the loading throughout the bed is within a few percent of the equilibrium loading by the end of the tests. Thus, the calculated

theoretical capacity is q_*/ρ_s; it falls within the uncertainty range of the measured values. This argues against any significant fraction of the sorbent in the bed being 'inactive' due to the presence of water. It is also possible that all of the CO_2 Toth isotherms for zeolites[11] were derived with sorbents that were contaminated with some unknown amount of H_2O due to too low of an activation temperature. This would make them inaccurate at low CO_2 loading levels.

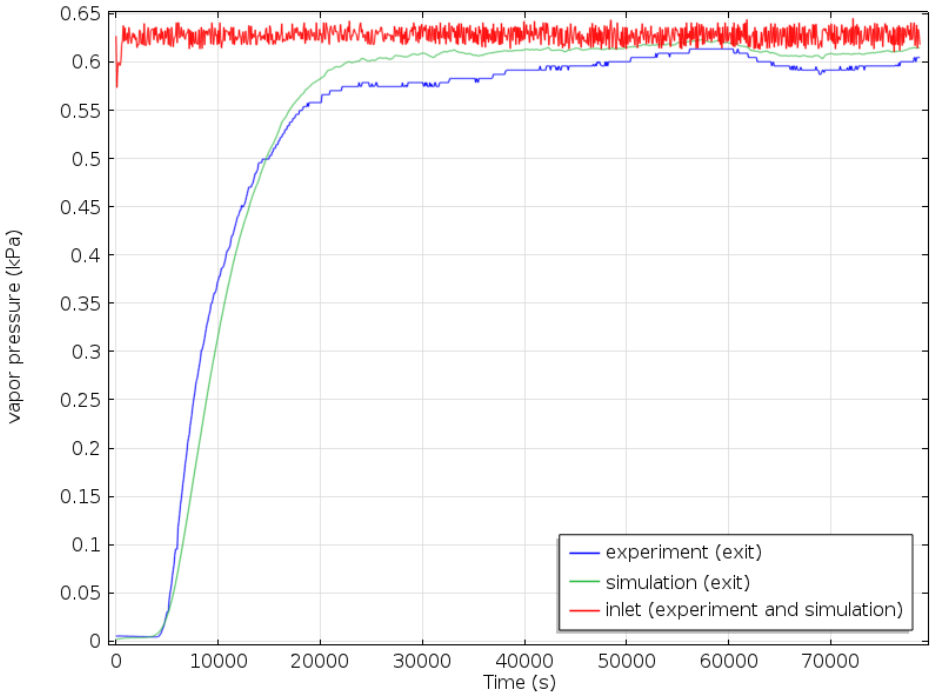

Figure 4. Water vapor pressures for SG Grade 40 with 16 SLPM and 0.5°C dew point.

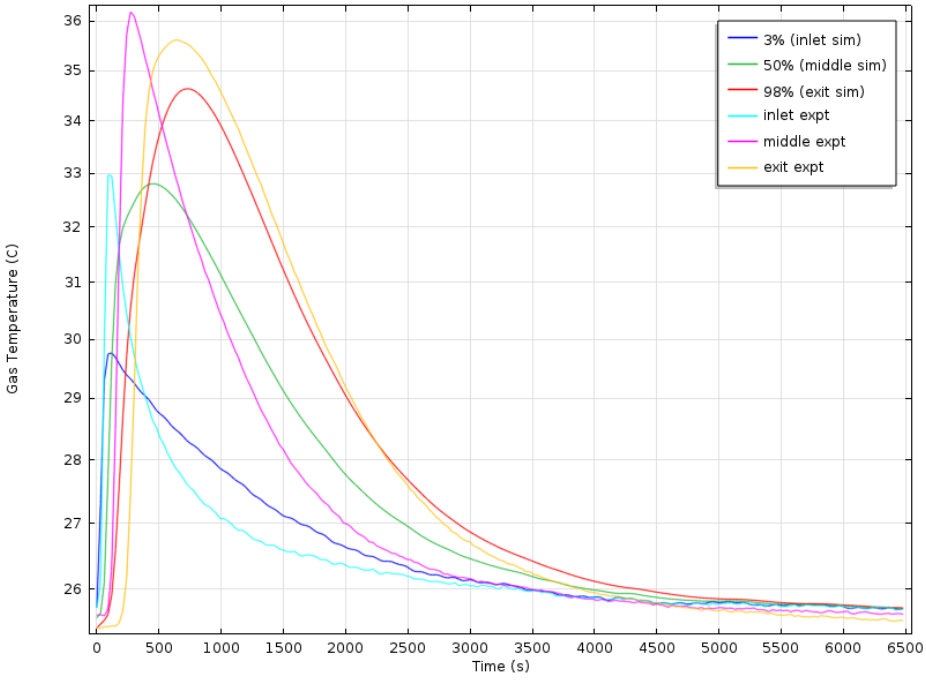

Figure 5. CO_2 temperatures for 5A RK38 at 16 SLPM with 5 Torr inlet partial pressure.

7. Conclusions

Using COMSOL, we have been able to derive a predictive model for adsorption physics in a variety of flow rate and sorbate partial pressure regimes and for a variety of sorbents. The limitations are in general due to the experimental data, not the model, due to variations and uncertainties in the dew point measurements, the ambient conditions, and unsteady flow conditions.

However, the model consistently underpredicts the temperature peaks and their falloff. This could be due to either inaccuracies in the isotherms at low loading or the correlations used for the heat transfer coefficients. Also, there are still deficiencies in the model, such as the LDF, which uses a single constant parameter to determine the loading rate. Further, the 1-D nature of the model is not capturing some of the physics due to channeling of the carrier gas near the walls of the sorbent bed. Future work will extend the PDEs used here to 2-D axisymmetry and will include the impact of using a radially dependent porosity due to packing. Since no purge gas is perfectly dry, another extension of this work is to include binary Toth relationships, particularly for the CO_2 tests, in order to properly capture the competition between H_2O and CO_2. The values of k_m found in this work will be used in broad applications of sorbent/sorbate systems to estimate performance without the need of testing.

8. References

[1]Perry, J. L., et, al., "Integrated Atmosphere Resource Recovery and Environmental Monitoring Technology Demonstration for Deep Space Exploration," *International Conference on Environmental Systems*. AIAA, San Diego, 2012.

[2]Knox, J.C., et. al., "Development of Carbon Dioxide Removal Systems for Advanced Exploration Systems," *International Conference on Environmental Systems*. AIAA, San Diego, 2012.

[3]COMSOL, COMSOL Multiphysics®, 2009.

[4]Rumpf, H., and Gupte, A.R., "The influence of porosity and grain size distribution on the permeability equation of porous flow", Chemie Ing. Techn. (Weinheim), v. 43, no. 6, p 367-375, 1975.

[5]Ergun, S., Chem. Eng. Prog., 48, 89, 1952.

[6]D. M. Ruthven, Principles of Adsorption and Adsorption Processes, Wiley Interscience: New York, 1984.

[7]M.F. Edwards and J.F. Richardson, Chem. Eng. Sci. 24, 607 (1969).

[8]Wakao, N. and Kaguei, S.1982 Heat And Mass Transfer In Packed Beds, Gordon and Breach, New York.

[9]Li, C.H., and Finlayson, B.A. 1977 Heat transfer in packed beds - a reevaluation Chem. Eng. Sci.32 1055-1066.

[10]E.L. Cussler, Diffusion: Mass Transfer in Fluid Systems, 2nd Edition (Cambridge University. Press, London, 1997.

[11]Wang, Y. and Levan, M.D. "Adsorption Equilibrium of Carbon Dioxide and Water Vapor on Zeolites 5A and 13X and Silica Gel: Pure Components", Journal of Chemical and Engineering Data, 54(10), 2839-2844, 2009.

[12]Ritter, J.A., and Ebner, A.D., "Design of an Adsorption-Based Carbon Dioxide, Humidity and Trace Contaminant Removal System", Final Report for Cooperative Agreement NNM05AA10A, 2008.

[13]"Davison Molecular Sieves Adsorption Equilibria", Davison Chemical Report.

[14]Yagi, S. and Kunii, D., "Studies on Heat Transfer Near Wall Surfaces in Packed Beds", AIChE J. 6 543-546, 1960.

[15]Kay, R., and Pancho, D., "Evaluation of Alternative Desiccants and Adsorbents for the Desiccant/Adsorbent Bed", Honeywell Report 12-77742, CAGE 70210, 2013.

[16]Finn, J.E., Ho, E.C., and Knox, J.C., "Progress Report on the 4BMS Adsorption Characterization Study", NASA Ames Research Center, 1995.

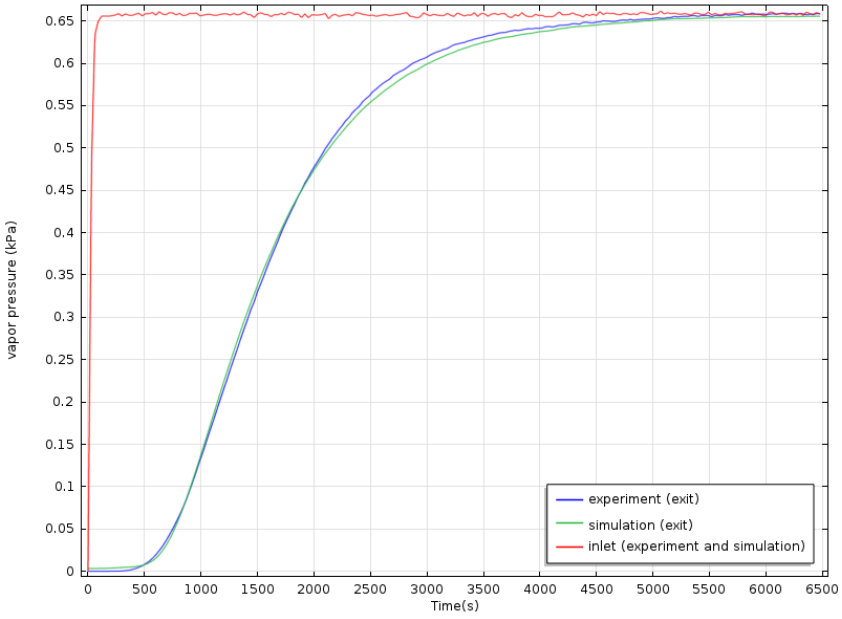

Figure 6. CO_2 partial pressures for 5A RK38 at 16 SLPM with 5 Torr inlet partial pressure.